

Monte Carlo studies of extensions of the Blume-Emery-Griffiths model

C. C. Loois, G. T. Barkema, and C. Morais Smith

Institute for Theoretical Physics, Utrecht University, Leuvenlaan 4, 3584 CE Utrecht, The Netherlands

(Received 15 August 2008; revised manuscript received 30 October 2008; published 25 November 2008)

We extend the Blume-Emery-Griffiths (BEG) model to a two-component BEG model in order to study two-dimensional systems with two order parameters, such as magnetic superconductors or two-component Bose-Einstein condensates. The model is investigated using Monte Carlo simulations, and the temperature-concentration phase diagram is determined in the presence and absence of an external magnetic field. This model exhibits a rich phase diagram, including a second-order transition to a phase where superconductivity and magnetism coexist. Results are compared with experiments on cerium-based heavy-fermion superconductors. To study cold-atom mixtures, we also simulate the BEG and two-component BEG models with a trapping potential. In the BEG model with a trap, there is no longer a first-order transition to a true phase-separated regime but a crossover to a kind of phase-separated region. The relation with imbalanced Fermi mixtures is discussed. We present the phase diagram of the two-component BEG model with a trap, which can describe boson-boson mixtures of cold atoms. Although there are no experimental results yet for the latter, we hope that our predictions could help to stimulate future experiments in this direction.

DOI: [10.1103/PhysRevB.78.184519](https://doi.org/10.1103/PhysRevB.78.184519)

PACS number(s): 67.85.Fg, 05.10.Ln

I. INTRODUCTION

Mixtures of ^3He and ^4He atoms exhibit a rich phase diagram, where besides a normal (N) phase, there is a phase where ^4He is superfluid and a phase-separated (PS) region of superfluid ^4He and normal ^3He .¹ In 1971, Blume, Emery, and Griffiths² (BEG) proposed a model to describe such mixtures. They simplified the continuous phase of the superfluid order parameter such that it could acquire only two values. Although they made this very rough approximation and modeled the uniform system in a lattice, their results are very interesting. Qualitatively, they reproduced the right phases and the right orders of the phase transitions. Furthermore, if disorder is introduced by placing the mixture into aerogel, after some modifications,³ the model can still yield the experimentally observed phase diagram.⁴

Here, we generalize this model to a two-component case in order to describe systems with two order parameters and study the problem numerically, using Monte Carlo simulations. The motivation for the model we are proposing is twofold. First, we would like to study condensed-matter materials such as heavy fermions, high- T_c superconductors, and organic superconductors. In particular, we want to study the interplay between magnetic and superconducting (S) ordering in these materials. Both order parameters are modeled as an Ising spin variable. Concerning the magnetism, we consider the ferromagnetic (FM) and the antiferromagnetic cases and investigate also the effect of an additional magnetic field. We find that in the absence of a magnetic field, in the region where the two orders coexist, the system is always phase separated. When we add a magnetic field, we also find regions with microscopic coexistence of the two phases. Second, we want to study mixtures of cold atoms. Cold atoms have emerged in recent years as an ideal simulator of condensed-matter systems. Because experiments with cold atoms are often carried out in a trap, we add a trapping potential to the model. This fact qualitatively changes the physics in the problem. For the case of a single-component

BEG model in a trap, the results are compared with experimental and theoretical work on imbalanced Fermi mixtures. For the case of the two-component BEG model, we make predictions for the phase diagram of boson-boson mixtures.

The outline of this paper is the following: in Sec. II, we introduce the two-component BEG model and investigate it in the presence and absence of an external magnetic field. The effect of a trapping potential is described in Sec. III. In Sec. IV, we compare the results with magnetic superconductors and cold-atom systems. Our conclusions are presented in Sec. V.

II. TWO-COMPONENT BLUME-EMERY-GRIFFITHS MODEL**A. Original Blume-Emery-Griffiths model**

A simple model for describing mixtures of bosonic and fermionic degrees of freedom, e.g., mixtures of ^3He - ^4He atoms, is the BEG model.² The ^4He atoms can be in a normal or in a superfluid phase, whereas the ^3He ones are in the normal phase. BEG introduced a crude but effective approximation, which can capture the essential features of the problem: the continuous superfluid order parameter describing the ^4He atoms is oversimplified using Ising spin variables. The phase of the wave function is therefore not allowed to take any value on the unit circle but just the values $S_i = \pm 1$. The remaining ^3He atoms are described by introducing a third value to the spin variable: $S_i = 0$.²

The model then consists of a fictitious spin variable S_i , which can take the values 0 and ± 1 on each site of a discrete lattice. Here we consider a two-dimensional (2D) lattice with N lattice points. There is only one atom per site and there are no vacancies. The ordering of S_i provides an order parameter for the model, allowing to describe transitions from the ferromagnetic (superfluid) phase to the paramagnetic (normal) phase. The number of ^3He and ^4He atoms is given by $N_3 = \sum_i (1 - S_i^2)$ and $N_4 = \sum_i S_i^2$. The total number of sites is

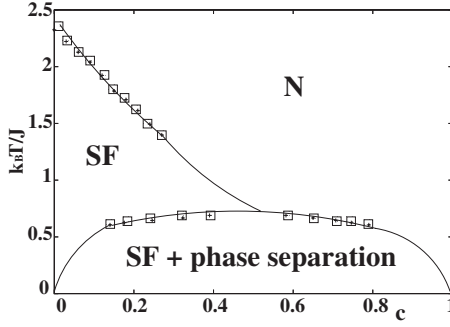


FIG. 1. Phase diagram of the original BEG model obtained by Monte Carlo simulations. N denotes the normal phase; SF denotes superfluidity. Lines are guides for the eyes. The transition between the normal and the superfluid state is second order; the transition to the phase-separated regime is first order.

given by $N=N_3+N_4$. The magnetization, which is given by the thermal average of the total spin $M=\sum_i\langle S_i\rangle/N$ provides an order parameter for superfluid ordering, whereas the concentration of ^3He $c=\langle N_3\rangle/N$ is an additional order parameter, which reflects the possibility of phase separation. The latter is given in terms of the mean quadrupole moment of the fictitious spin system $Q=\sum_i\langle S_i^2\rangle/N$, i.e., $c=1-Q$. Hence, superfluid ordering and phase separation in the ^3He - ^4He mixtures are simulated, respectively, by magnetic ordering and quadrupolar ordering in the BEG model.

The Hamiltonian of the BEG model reads as

$$\mathcal{H}_{\text{BEG}} = -J \sum_{\langle ij \rangle} S_i S_j + \kappa \sum_{\langle ij \rangle} S_i^2 S_j^2 + D \sum_i S_i^2. \quad (1)$$

Here, $\langle i, j \rangle$ denotes nearest-neighbor pairs, J is the exchange interaction, κ is the biquadratic exchange, and D denotes the crystal field, which incorporates the chemical potentials μ_3 and μ_4 for ^3He and ^4He .

Initially, BEG solved the Hamiltonian (1) without the biquadratic exchange interaction, i.e., at $\kappa=0$. In this limit their model reduces to the Blume-Capel model.⁵ The phase diagram of the latter is shown in Fig. 1. The first term in the Hamiltonian (1) then leads to superfluid ordering below a critical temperature T_c , which depends on the exchange interaction J and on the concentration c of ^3He atoms. If the temperature is sufficiently low and c is sufficiently large, the system separates into two phases: one which is superfluid and poor in ^3He atoms and another one which is normal and rich in ^3He atoms. This is equivalent to quadrupolar ordering in the BEG model.

This area of research has been very active (see, e.g., Ref. 6 and references therein). The BEG model has been studied with a general κ (see Refs. 7 and 8); variations in this model have been investigated to describe Ising magnets with mobile defects⁹ and long- and short-range interactions have been included.¹⁰

Although here we will be concerned with extensions of the Blume-Capel model Hamiltonian,⁵ we will nevertheless keep the reference to BEG because the main assumption of our model relies on their original proposal of projecting the phase of the wave function. It is interesting that in spite of

this very bold approximation, the phase diagram of the BEG model (Blume-Capel Hamiltonian with the phase projection) found by Monte Carlo simulations (see Fig. 1) exhibits large similarities with the phase diagram of ^3He - ^4He mixtures measured by experimentalists.¹ This agreement is the motivation for the model we propose below.

B. Model

The main idea of studying superfluidity with the BEG model relies on the $U(1)$ symmetry breaking of the ground-state wave function. For superconductivity and Bose-Einstein condensation we have the same symmetry breaking; hence we can try to model these phenomena in the same way.

Several physical systems exhibit two unequal symmetry-broken phases simultaneously. A general Hamiltonian describing this class of systems reads as

$$\mathcal{H} = -J_1 \sum_{\langle ij \rangle} \sigma_i \sigma_j - J_2 \sum_{\langle ij \rangle} s_i s_j + D \sum_i \sigma_i^2 + H \sum_i \sigma_i, \quad (2)$$

where J_1 and J_2 are the exchange interactions for σ -type and s -type bosons, respectively, D is an anisotropy field that controls the number of lattice sites with nonzero σ_i , and H plays the role of an external magnetic field, which may couple only to the order parameter describing a magnetic transition. Here, we consider a 2D lattice and assume that the “spins” (σ_i, s_i) can take the values $(0,1)$, $(0,-1)$, $(1,0)$, and $(-1,0)$. This choice implies that only one kind of boson can occupy each lattice site, i.e., we are implicitly assuming the constraint $s_i^2 + \sigma_i^2 = 1$ at each lattice site i . Notice that in the original (one-component) BEG model, every site is occupied either by a fermion ($\sigma=0$) or by a boson ($\sigma=\pm 1$) and there is no constraint. In the two-component BEG model considered here, every site is occupied either by a boson of type $s=\pm 1$ or a boson of type $\sigma=\pm 1$. In this case, $s=0$ or $\sigma=0$ means that this site is not occupied by a boson of s or σ type. Therefore, the constraint $s_i^2 + \sigma_i^2 = 1$ implies that every site is only occupied by one type of boson and there are no fermions in the problem.

The Hamiltonian (2) is appropriate for describing phase transitions which require two order parameters: one describing the ordering of the fraction of the system with nonzero σ and the other one with nonzero s . This yields several possibilities; both fractions can model superfluidity, superconductivity, or (anti)ferromagnetism. Possible applications could be magnetic superconductors or two-component Bose-Einstein condensates.

From now on, we will consider the fraction with non-negative σ as describing magnetism and s superconductivity (preformed bosons that can Bose-Einstein condensate). Thus, σ_i represents the spin of particle i and s_i represents the discretized phase of the wave function. Therefore, J_1 can be both positive (ferromagnetism) and negative (antiferromagnetism), but J_2 has to be positive. We define the concentration, the ferromagnetic, antiferromagnetic, and superconducting order parameters as

$$c = \frac{1}{N} \sum_i \sigma_i^2, \quad (3)$$

$$m_{\text{fm},\sigma} = \frac{1}{N} \sum_i \sigma_i, \tag{4}$$

$$m_{\text{af},\sigma} = \frac{1}{N} \sum_i (-1)^i \sigma_i, \tag{5}$$

$$m_s = \frac{1}{N} \sum_i s_i. \tag{6}$$

Note that $m_{\text{fm},\sigma}$ and $m_{\text{af},\sigma}$ can reach a maximum value of c and m_s can reach a maximum value of $1-c$. We define the ratio between the two coupling constants J_2 and J_1 as

$$K = \frac{J_2}{|J_1|}. \tag{7}$$

Although we restrict our investigation to the simplest possible model including two order parameters, extensions involving an interaction between the latter could be envisaged, e.g.,

$$H_{\text{int}} = -J_3 \sum_{\langle ij \rangle} \sigma_i \cdot s_j. \tag{8}$$

This term would allow us to address issues such as the competition between singlet or triplet superconductivity in the presence of ferromagnetism. Although very interesting and certainly relevant to provide a more realistic description of several heavy-fermion superconductors, this term will nevertheless be put to zero in our present studies.

C. Method

We investigate the two-component BEG model in a 2D lattice by Monte Carlo simulations. To determine the location of second-order phase transitions, we performed simulations at constant concentration, in which the elementary moves were flips of s_i and σ_i or nonlocal spin exchanges. The location of the transition is then obtained from the peak location of the magnetic susceptibility. The locations of first-order phase transitions are obtained from simulations at constant temperature. The elementary moves are local flips of s_i and σ_i , as well as same-site replacements of s_i by σ_i and vice versa. A jump in the concentration c as a function of the anisotropy field D is then the signature of the phase transition (see Fig. 2, where this jump can be visualized for the case of the original BEG model).

All simulations are performed on lattices with approximately 40×40 sites. Per point in the phase diagram, simulations were run over $3 \times 10^5 - 3 \times 10^7$ Monte Carlo steps per site, depending on the correlation times.

D. Zero magnetic field, $H=0$

In the absence of a magnetic field, the Hamiltonian (2) has ferro-antiferromagnetic symmetry.

First, we consider $K=1$. In this case, $J_1=J_2$, and the shape of the phase diagram must be symmetric under the transformation $c \rightarrow 1-c$. The results of the simulations are plotted in Fig. 3. We see that it indeed obeys this symmetry and exhib-

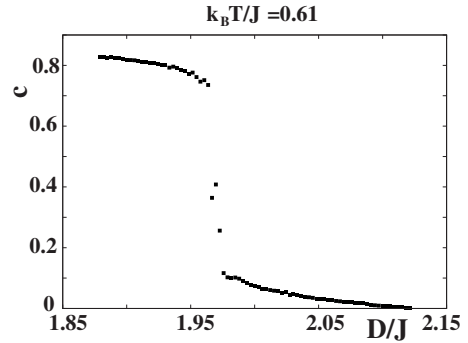


FIG. 2. Concentration of ^3He as a function of the anisotropy field D for the original BEG model for $k_B T/J=0.61$. At $(D/J)_c \approx 1.97$, this concentration makes a jump, indicating a first-order phase transition.

its four phases: a S phase, where the order parameter m_s is nonzero; a FM phase, where $m_{\text{fm},\sigma}$ is nonzero; a PS regime where the spins and the angular phases have formed ordered clusters, and finally the N phase, in which there is neither order nor phase separation. Analogous to the BEG model, the transition from the phase-separated regions to other phases are first order (dashed line); the other ones are second order (continuous line).

Second, we consider the case $K=0.1$. The results of the simulations are plotted in Fig. 4. We can understand the results as follows: J_2 is much smaller than J_1 ; hence the spins will not pay much attention to the angular phases, and the part of the phase diagram concerning the spins will be very similar to the BEG model. Because J_2 is so small, the phases will only order at very low temperatures (at zero concentration, the temperature is ten times lower than the one at which the spins order at a concentration of one). If the concentration is slightly raised from zero, the system is already in the phase-separated regime. All the states with a nonzero phase have clustered and are not diluted by states with nonzero spin. Therefore, the critical temperature in the phase-separated region will approximately remain constant. Be-

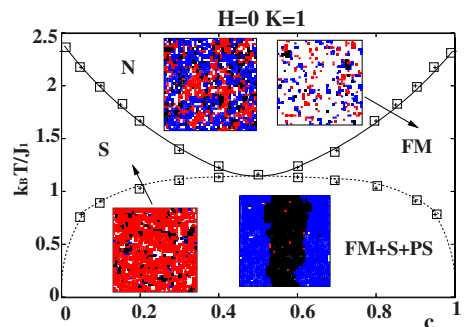


FIG. 3. (Color online) Phase diagram for temperature (in units of J_1/k_B) versus concentration in the absence of a magnetic field, for a relative coupling constant of $K=1$. N, S, FM, and PS indicate the normal phase, superconductivity, ferromagnetism, and phase separation, respectively. Solid lines represent second-order phase transitions; dashed lines represent first-order ones. Lines are guides for the eyes. Snapshots of the simulation are shown. Black (white) represents $\sigma_i=1$ (-1); red (blue) represents $s_i=1$ (-1).

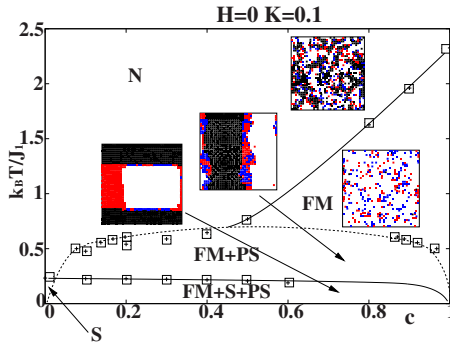


FIG. 4. (Color online) Phase diagram for temperature (in units of J_1/k_B) versus concentration in the absence of a magnetic field, for a relative coupling constant of $K=0.1$. N, S, FM, and PS indicate the normal phase, superconductivity, ferromagnetism, and phase separation, respectively. Solid lines represent second-order phase transitions; dashed lines represent first-order ones. Lines are guides for the eyes. Snapshots of the simulation are shown. Black (white) represents $\sigma_i=1$ (-1); red (blue) $s_i=1$ (-1). Notice that superconductivity and phase separation do not set in at the same temperature.

cause the temperature at which the angular phases order is lower than the temperature at which phase separation begins, there is a phase-separated region in which the angular phases of the wave function are not ordered, which may appear unexpected at first sight. The transition within the phase-separated regime, from the region where the angular phases are not ordered to the phase where they are ordered (superconductivity), is second order. This is expected because in the phase-separated regime, all the phases have clustered and the transition will be comparable with the transition in the Ising model, which is also second order. Notice that although the region where superconductivity sets in shrinks with decreasing K , there is no critical K below which the superconducting phase completely disappears. At the concentration $c=0$ the model reduces to the Ising model, and thus there is a critical temperature for superconductivity of $k_B T/J \approx 2.4$ at this concentration.

E. Adding a magnetic field: The antiferromagnetic case

If we apply a non-negative uniform magnetic field to the system, the ferro-antiferromagnetic symmetry is broken. We choose to consider the antiferromagnetic case here because then there are two competing effects: the magnetic field tends to align the spins, whereas the exchange interaction wants to order the spins antiferromagnetically. The magnetic field H will be measured in units of J_1 .

Kimel *et al.*¹¹ studied the antiferromagnetic BEG model in the presence of a magnetic field using Monte Carlo simulations. Their results at zero temperature suggest that the behavior of the system should be separated into three qualitatively distinct regions, namely, $H \in [0, 2]$, $H \in [2, 4]$, and $H \in [4, \infty]$. We consider here the cases $K=1$ and 0.1 for values of H within each of these intervals.

1. $H=1.5$

First, we consider a magnetic field in the interval $[0, 2]$, namely, $H=1.5$. Both for $K=1$ and 0.1 , the results (not

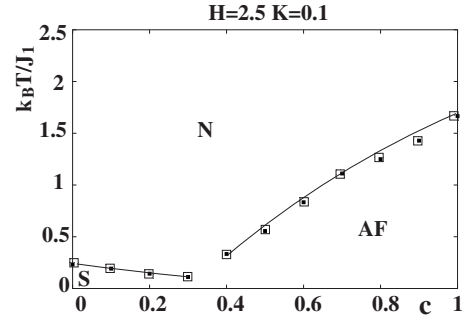


FIG. 5. Phase diagram for temperature (in units of J_1/k_B) versus concentration at a magnetic field $H=2.5$ and at a relative coupling constant $K=0.1$. N, S, and AF denote the normal phase, superconductivity, and antiferromagnetism, respectively. Solid lines represent second-order phase transitions and the lines are guides for the eyes.

shown) are qualitatively the same as in the case of $H=0$. This behavior was expected from the phase diagram of the single-component BEG model at zero temperature. Because the magnetic field tries to align the spins, the antiferromagnetic transition temperature is lower than in the absence of a magnetic field.

2. $H=2.5$

In the usual BEG model, the first-order phase transition disappears in the presence of a magnetic field $H \in [2, 4]$. At zero temperature, there is a second-order phase transition between a state with $\sigma_i=0$ at every site and a checkerboard phase, where one sublattice has $\sigma_i=0$ at every site and the other one has $\sigma_i=-1$. There is also a transition between the checkerboard state and an antiferromagnetic phase, but this transition is absent at nonzero temperature.¹¹

For $K=1$, the behavior of the two-component BEG model is still very similar to the case $H=0$. For $K=0.1$, the first-order phase transition disappears and therefore there is no phase-separated region (see Fig. 5). We do observe an antiferromagnetic and a superconducting phase, but it is not clear from the figure whether the two phases overlap. To better understand this low- T intermediate regime, we also simulated the problem at a relative coupling strength of $K=0.5$. In Fig. 6, we clearly observe that there is a region where antiferromagnetism and superconductivity coexist, *without true phase separation*, since the first-order phase transition has disappeared.

3. $H=5$

In the original BEG model, when the magnetic field is increased to a value higher than $H=4$ at zero temperature, antiferromagnetism totally disappears because the spins tend to align with the magnetic field.¹¹ The system is therefore magnetized, but not because of the nearest-neighbor interactions. Therefore, this is not really ferromagnetism; but for the sake of simplicity, we denote it like this. For the case of $K=1$, we observe a phase with ferromagnetic and superconducting ordering and a ferromagnetic phase (not shown). For $K=0.1$, we find another interesting phase, namely, a ferro-

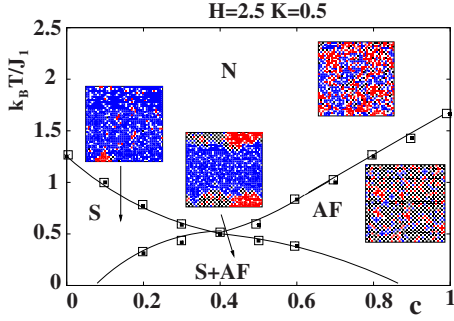


FIG. 6. (Color online) Phase diagram for temperature (in units of J_1/k_B) versus concentration at a magnetic field $H=2.5$ and at a relative coupling constant $K=0.5$. N, S, and AF denote the normal phase, superconductivity, and antiferromagnetism, respectively. There is a region where superconductivity and antiferromagnetism coexist, but where there is no true phase separation. Solid lines represent second-order phase transitions and lines are guides for the eyes. Snapshots of the simulation are shown. Black (white) represents $\sigma_i=1$ (-1); red (blue) $s_i=1$ (-1).

magnetic checkerboard phase, consisting of two sublattices (see Fig. 7). At the first sublattice, all sites are randomly occupied by phases with a value of $s_i=1$ or $s_i=-1$. At the second one, all sites are occupied by the spin that is favored by the magnetic field $\sigma_i=-1$. This phase is most likely to occur at a concentration of $c=0.5$ because in this case a perfect checkerboard is possible.

III. ADDING A TRAP POTENTIAL

A. Blume-Emery-Griffiths model

Because experiments with cold atoms are often carried out in a trap, we will add a harmonic potential to the original 2D BEG Hamiltonian to describe mixtures of fermions and bosons in a trap. In general, the potential felt by the bosons is different from the one felt by the fermions, which implies that we must include two terms,

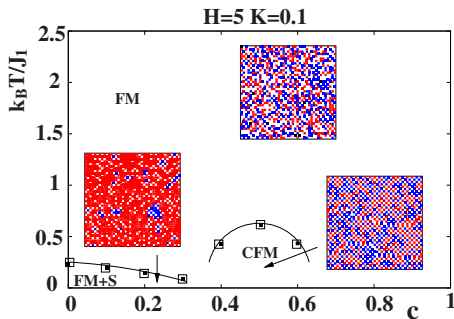


FIG. 7. (Color online) Phase diagram for temperature (in units of J_1/k_B) versus concentration at $H=5$ and at $K=0.1$. FM denotes ferromagnetism, S denotes superconductivity, and CFM denotes checkerboard ferromagnetism. Solid lines represent second-order phase transitions and lines are guides for the eyes. Snapshots of the simulation are shown. Black (white) represents $\sigma_i=1$ (-1); red (blue) $s_i=1$ (-1).

$$a_b \sum_i (x_i^2 + y_i^2) \sigma_i^2 + a_f \sum_i (x_i^2 + y_i^2) (1 - \sigma_i^2). \quad (9)$$

Here, x_i and y_i are the horizontal and vertical distances of site i measured from the center of the lattice, in lattice units, and a_b and a_f measure how much the bosons (the states with $\sigma_i = \pm 1$) and the fermions (the states with $\sigma_i = 0$) feel the influence of the trap. If $a_b = a_f$, this term is constant, and the phase diagram is not modified. We will consider the case $a_b > a_f$, which is the most relevant experimentally. We can then rewrite Eq. (9) and add it to the BEG Hamiltonian, thus obtaining

$$\mathcal{H} = -J \sum_{\langle ij \rangle} \sigma_i \sigma_j + D \sum_i \sigma_i^2 + a \sum_i (x_i^2 + y_i^2) \sigma_i^2, \quad (10)$$

where $a = a_b - a_f$. This means that effectively, the bosons will feel a stronger tendency to go to the center of the trap.

In the limit of $a \rightarrow \infty$, all the states with $\sigma_i = \pm 1$ will cluster in the center of the trap, and therefore the ordering temperature will be the same as in the Ising model. Note that the maximum value of the extra term in the Hamiltonian will depend on the size of the lattice. This way of including the trapping potential is comparable with the work of Gygi *et al.*,¹² where a spatial-dependent chemical potential was added to the Bose-Hubbard model in order to describe bosonic atoms in an optical lattice.

We simulated this model using the same procedures as for the original BEG model and the two-component BEG model. The results for three different strengths of the trapping potential are plotted in Fig. 8. In the BEG model without a trap, there is a second-order phase transition from a normal state to an ordered state and a first-order phase transition to a phase-separated region.² For the three values of a considered here, we do not find a first-order phase transition any more. A part of the first-order phase-transition line disappears and a part changes into a second-order one.

We see that for a small difference between the trap potential felt by the bosons and the fermions, $a/J=0.001$, the transition temperatures are very similar to the case without a trap. For a large difference, $a/J=0.1$, the transition temperatures approach the transition temperature of the Ising model for almost all concentrations, as expected. When the states with $\sigma_i = \pm 1$ are ordered, we will not speak of a superfluid state but of a condensed state because we now consider bosons in general.

It is important to estimate at which temperature the system starts to feel the influence of the trapping potential. Let us assume that a cluster of size m feels the potential when the energy difference between the state with this cluster in the center and in the corner of the lattice is of the order $k_B T / J$. For a lattice of size L^2 , this estimation results in

$$\frac{m a L^2}{2J} \sim \frac{k_B T}{J}. \quad (11)$$

In this approximation, a single particle ($m=1$) in a lattice of size $L=41$ will start to feel the potential if $k_B T / J \sim 800a$. For $a/J=0.1$ and 0.01 this results in $k_B T / J \sim 80$ and $k_B T / J \sim 8$, respectively, in both cases much higher than the temperatures we are interested in because ordering starts around

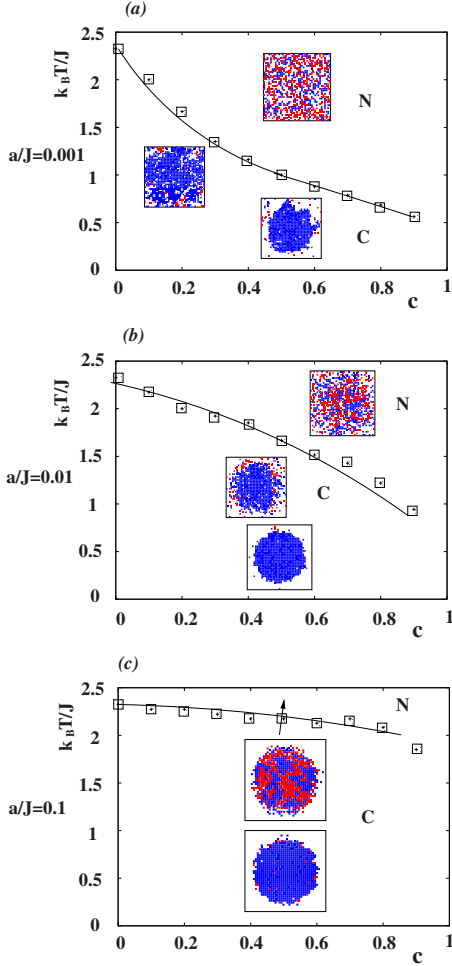


FIG. 8. (Color online) Phase diagrams of the original BEG model with a trapping potential, showing temperature (in units of J/k_B) versus concentration. N denotes the normal unordered state and C the condensed phase, in which the sites with $\sigma_i = \pm 1$ are ordered. Lines are guides for the eyes and represent second-order phase transitions. Snapshots are shown, where blue represents $\sigma_i = 1$, red represents $\sigma_i = -1$, and white represents $\sigma_i = 0$. The parameter $a = a_b - a_f$ measures the difference in the intensity of the trapping potential felt by the bosons and the fermions. (a) $a/J = 0.001$; (b) $a/J = 0.01$; and (c) $a/J = 0.1$.

$k_B T/J \approx 2.4$. Therefore, the single particles will experience the influence of the trap in the entire temperature range of Figs. 8(b) and 8(c). For $a/J = 0.001$, a single particle will feel the trapping potential for temperatures lower than $k_B T/J \sim 0.8$. However, for higher temperatures the system already orders, and therefore there are some large clusters that according to Eq. (11) will feel the potential already at much higher temperatures. This reasoning is in agreement with the snapshots in Fig. 8(a). For $a/J = 0.001$, we clearly observe the influence of the trap when the states with $\sigma_i = \pm 1$ have clustered. In the disordered state, the influence is less visible. For $a/J = 0.1$ and 0.01 , we indeed see the influence of the trap for all temperatures, even in the disordered state.

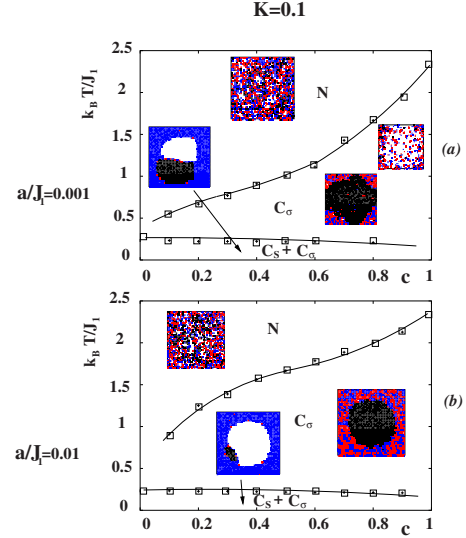


FIG. 9. (Color online) Phase diagrams of the two-component BEG model with a trapping potential, showing temperature (in units of J_1/k_B) versus concentration for a relative coupling constant $K = 0.1$. N denotes the normal unordered state; C_σ and C_s denote the phases where the bosons represented by the state with $\sigma_i = \pm 1$, respectively, $s_i = \pm 1$ are condensed. Lines are guides for the eyes and represent second-order phase transitions. Snapshots are shown, where black and white represent $\sigma_i = \pm 1$, and red and blue represent $s_i = \pm 1$. The parameter $a = a_\sigma - a_s$ measures the difference between the potentials felt by the two species of bosons. (a) $a/J_1 = 0.001$; (b) $a/J_1 = 0.01$.

B. Two-component Blume-Emery-Griffiths model

Analogous to Sec. III A, we will also add a trapping potential to the 2D two-component BEG model. In the latter, both the states with $\sigma_i = \pm 1$ and $s_i = \pm 1$ describe bosons that both can condense. Therefore, this model can be applied to study cold-atom mixtures with two species of bosons. We will consider the realistic case that the two species feel different trapping potentials. Therefore, we add the extra terms

$$a_\sigma \sum_i (x_i^2 + y_i^2) \sigma_i^2 + a_s \sum_i (x_i^2 + y_i^2) s_i^2 \quad (12)$$

to the Hamiltonian. Because at every lattice site $\sigma_i^2 + s_i^2 = 1$, we can rewrite this term and add it to the two-component BEG Hamiltonian to get

$$\mathcal{H} = -J_1 \sum_{\langle ij \rangle} \sigma_i \sigma_j - J_2 \sum_{\langle ij \rangle} s_i s_j + D \sum_i \sigma_i^2 + a \sum_i (x_i^2 + y_i^2) \sigma_i^2, \quad (13)$$

where $a = a_\sigma - a_s$ is now the difference between the potentials felt by the two species of bosons. Now, the bosons with $\sigma_i = \pm 1$ have a stronger tendency to go to the center of the lattice.

The results of our simulations are plotted in Figs. 9 and 10. We considered two different strengths of the trapping potential and two different ratios of the coupling strengths of the bosons, namely, $K = J_2/J_1 = 1$ and $K = 0.1$. For $K = 0.1$, the right part of the first-order phase transition disappears and the left one becomes second order (see Fig. 9); whereas for

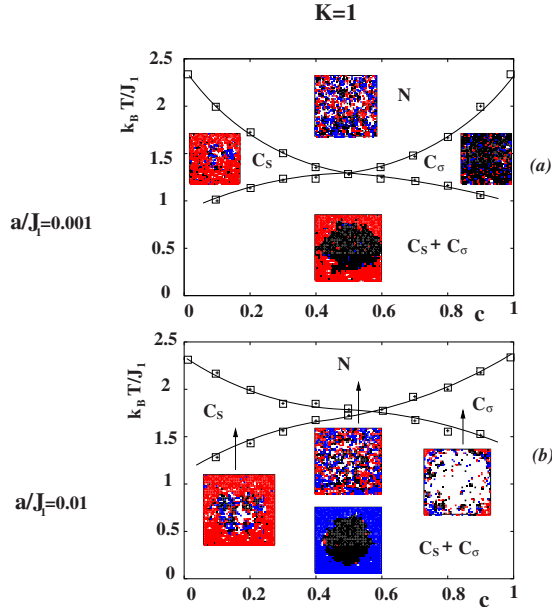


FIG. 10. (Color online) Phase diagrams of the two-component BEG model with a trapping potential, showing temperature (in units of J_1/k_B) versus concentration for a relative coupling constant $K=1$. N denotes the normal unordered state; C_σ and C_s denote the phases where the bosons represented by the state with $\sigma_i = \pm 1$, respectively, $s_i = \pm 1$ are condensed. Lines are guides for the eyes and represent second-order phase transitions. Snapshots are shown, where black and white represent $\sigma_i = \pm 1$, and red and blue represent $s_i = \pm 1$. The parameter $a = a_\sigma - a_s$ measures the difference between the potentials felt by the two species of bosons. (a) $a/J_1 = 0.001$; (b) $a/J_1 = 0.01$.

$K=1$ both left and right parts of the first-order phase transition are converted into second order (see Fig. 10).

In the limit of $a \rightarrow \infty$, all the sites with $\sigma_i = \pm 1$ will have clustered in the center of the lattice and all sites with $s_i = \pm 1$ will have clustered at the corners. Therefore, for all concentrations, the system behaves as two uncoupled Ising models. In the case of $K=1$, we see indeed that the transition temperatures for both species approach the Ising transition temperature. For $K=0.1$, because J_2 is ten times smaller than J_1 , one of the species will order at the Ising transition temperature and the other one at one tenth of the Ising transition temperature.

To find the temperature at which the system starts to feel the presence of the trap, we can make the same analysis as in Sec. III A. Also here, we see in the snapshots of Figs. 9 and 10 that for $a/J_1 = 0.1$ (not shown) and $a/J_1 = 0.01$, the system always feels the influence of the trap and for $a/J_1 = 0.001$, it does only when the system is ordered. If we inspect Fig. 10(a), we see that there is a phase C_s in which the bosons represented by $s_i = \pm 1$ are ordered, but the bosons represented by $\sigma_i = \pm 1$ are not. This is somewhat surprising. A reason for the occurrence of this phase is that when all the bosons that have the tendency to go to the center of the trap have clustered there, automatically also the other bosons have clustered at the edge. Therefore, they can have nearest-neighbor interactions and they can easily order. It remains to be seen whether such a phase indeed occurs in experiments.

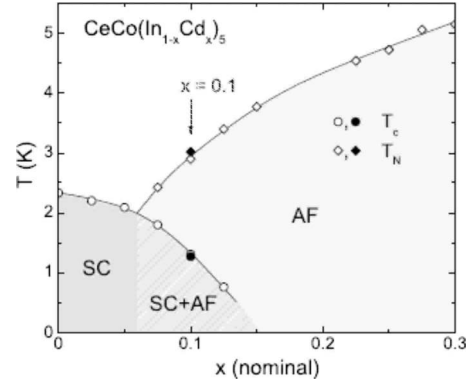


FIG. 11. Phase diagram temperature versus doping of $\text{CeCo}(\text{In}_{1-x}\text{Cd}_x)_5$. AF denotes antiferromagnetism and SC denotes superconductivity. The figure is extracted from Ref. 14.

From the theoretical point of view, it would be interesting to also allow for states with $\sigma_i = s_i = 0$ to verify the stability of this phase, when we relax the constraint that every lattice site must be occupied by one of the bosons. Note that for small enough concentrations, this phase will always occur since the bosons s are hardly diluted by the bosons σ .

IV. COMPARISON WITH EXPERIMENTS

A. Magnetic superconductors

There are several examples of cerium-based superconductors, for example, CeCoIn_5 and CeIrIn_5 , as well as antiferromagnets that contain this element, such as CeRhIn_5 , CeCoCd_5 , CeRhCd_5 , and CeIrCd_5 . Let us consider CeCoIn_5 and CeCoCd_5 . These two materials have two elements in common (Ce and Co) and differ in the third element. By doping CeCoIn_5 with Cd on the In site, we can change the superconductor CeCoIn_5 into an antiferromagnet. There are more of these cerium-based pairs, and therefore, this class of materials is appropriate for studying the interplay between superconductivity and magnetism.

Let us consider the heavy-fermion superconductor CeCoIn_5 , with cadmium doping on the In site. This material has the highest superconducting transition temperature ($T_c = 2.3$ K) of all heavy fermions, and its electronic structure is quasi-2D.¹³ Nicklas *et al.*¹⁴ and Pham *et al.*¹⁵ determined the antiferromagnetic and superconducting onset temperatures of this material as a function of doping by elastic neutron-scattering, specific-heat, and resistivity measurements. Their results are plotted in Fig. 11. For experimental details we refer the reader to Ref. 14. The phase diagram of $\text{CeCo}(\text{In}_{1-x}\text{Cd}_x)_5$ shows three ordered phases: a superconducting phase, a commensurate antiferromagnetic phase, and a region where superconductivity and antiferromagnetism microscopically coexist.

It is interesting to observe that in this material antiferromagnetism suddenly disappears at the point where the onset temperatures for superconductivity and antiferromagnetism are equal. This feature, however, may change in the presence of an applied magnetic field. In Fig. 12 we see a schematic phase diagram of unconventional superconductors in

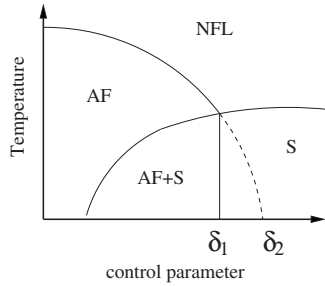


FIG. 12. Schematic phase diagram of unconventional superconductors in temperature versus control-parameter space. AF denotes antiferromagnetism, S denotes superconductivity, and NFL denotes a non-Fermi liquid. Experimentally, antiferromagnetism often disappears abruptly at some critical value δ_1 of the control parameter, although one would expect a magnetic quantum critical point at some value δ_2 of the control parameter.

temperature-control parameter space. In the case of $\text{CeCo}(\text{In}_{1-x}\text{Cd}_x)_5$, the control parameter would be doping. Another example of such a parameter is pressure. Park *et al.*¹⁶ determined the phase diagram of CeRhIn_5 in temperature-pressure space with and without a magnetic field. Without a magnetic field, they also found this abrupt disappearance of the incommensurate antiferromagnetic order at δ_1 . However, when they applied a field of 33 kOe, the line of the magnetic ordering temperature went smoothly down to zero at δ_2 . Such a phase diagram shows many similarities with Fig. 6 if we identify pressure with inverse concentration in our model. Indeed, for an external magnetic field of $H=2.5$ and a relative coupling constant $K=0.5$ (see Fig. 6), the phase diagram shows the same three ordered phases. Further, the coexisting phase is not phase separated.

Finally, we consider the compound $\text{CeIr}(\text{In}_{1-x}\text{Cd}_x)_5$ (see Fig. 13 and Ref. 15). For this material, it is not clear if there is a region where superconductivity and magnetism coexist. If there is such a region, it is in a small doping interval. The phase diagram of this material strongly resembles the phase diagram of the two-component BEG model with an external magnetic field of $H=2.5$ and a relative coupling strength of $K=0.1$ (see Fig. 5). Although this experiment was also carried out without an external magnetic field, we only find similarities with our model in the presence of a magnetic field.

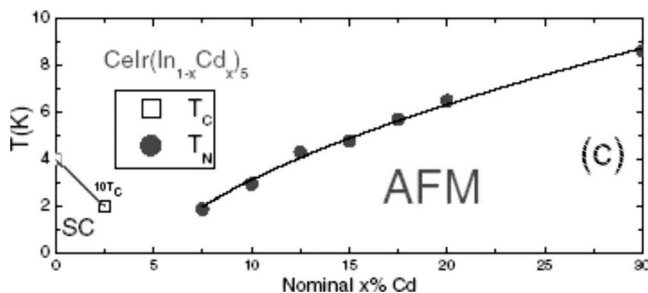


FIG. 13. Phase diagram temperature versus cadmium doping of the heavy fermion $\text{CeIr}(\text{In}_{1-x}\text{Cd}_x)_5$. SC denotes superconductivity and AFM denotes antiferromagnetism. The figure is extracted from Ref. 15.

B. Cold-atom systems

In 2006, two experimental groups, Ketterle and co-workers¹⁷ at MIT and Hulet and co-workers¹⁸ at Rice University, performed experiments with imbalanced ultra-cold ^6Li atoms in a trap and obtained results which seemed to be contradictory at first sight. The MIT group measured a transition between a normal and a superfluid phase at a polarization of $P \approx 0.70$, whereas the group at Rice University observed a transition between two superfluid phases at $P \approx 0.09$. Here, P measures the imbalance between the spin-up and the spin-down atoms,

$$P = \frac{N_{\uparrow} - N_{\downarrow}}{N_{\uparrow} + N_{\downarrow}}. \quad (14)$$

Gubbels *et al.*¹⁹ set up a theoretical model to describe these imbalanced Fermi mixtures and determined a general phase diagram in temperature-polarization space that can explain the observations of both groups. The topology of their phase diagram shows large similarities with the phase diagram of the BEG model. We can understand this resemblance as follows. In the BEG model, the concentration c is the fraction of lattice sites with $\sigma_i=0$ and thus the fraction of the system that cannot condense. The polarization P is a measure for the difference of the atoms in the spin-up and the spin-down states and thus for the number of fermions that remain after the others have paired. The atoms with spin up and spin down will form pairs and such a pair can be described as a boson. Therefore, the polarization is also a measure for the fraction of the system that cannot condense, and the concentration can be mapped onto the polarization. We can identify the paired atoms (bosons), with the states $\sigma_i = \pm 1$ and the remaining fermions with $\sigma_i=0$; see Fig. 1.

The experiments with ^6Li are carried out in a trap, and the theoretical model of Gubbels *et al.*¹⁹ only included the presence of the trap by using the local-density approximation. Now, we would like to compare their phase diagram with our results of the BEG model with a trapping potential in Figs. 9 and 10. Although in the case of imbalanced fermions the frequency ω of the optical trap felt by the pairs of fermions (bosons) and the remaining unpaired fermions is the same, the mass of the bosons is twice as large and the potential constant a_b is thus larger than a_f . This means that the comparison must be made with the BEG model in a trap. In this model, the first-order phase transition measured by a jump in the concentration as a function of the anisotropy field D has disappeared, thus there is no true transition to a phase-separated regime. However, if we inspect the snapshots, we see that for low enough temperatures or large enough trapping potential, there still is a clear separation between the condensed bosons and the fermions, suggesting some kind of effective phase separation. We note that in experiments, phase separation is measured by inspecting the radii of the clouds of the atoms in the different hyperfine states and not by a jump in some order parameter.¹⁸ Our results thus suggest that the measured different radii are not *per se* an evidence of a true thermodynamic phase separation. Further experiments are required to clarify this issue.

Although our model describes qualitatively the experimentally observed phases, it cannot capture the fine details of recent experimental results. Studies by Shin *et al.*²⁰ indicated that there is no superfluid phase or phase-separated phase for polarizations above $P \approx 0.36$. By a quantum Monte Carlo approach, Lobo *et al.*²¹ predicted a phase transition between a normal and a superfluid state at a polarization of $P \approx 0.39$ at zero temperature, and Gubbels and Stoof²² recovered these results using a Wilsonian renormalization-group theory.

V. CONCLUSIONS

We simulated a two-component extension of the 2D BEG model without an external magnetic field and determined the phase diagram in the concentration-temperature space. In the region where magnetism and superconductivity coexist, the system is always phase separated. We added a magnetic field to our model and considered the antiferromagnetic case. In this case, we also find phase diagrams with true coexistence of two ordered phases. These diagrams are comparable with the phase diagram of doped heavy fermions in the presence of a magnetic field.

In order to describe cold-atom systems, we added a trapping potential to the BEG model and our extension of this model. The added potential changes the phase-separation regime conceptually. We cannot speak anymore about true phase separation but more about a crossover to a phase-separated region. We argue that the BEG model with a trapping potential can be used to model imbalanced Fermi mixtures. However, there are still quantitative differences with experiments, which our model is not able to cover. We also made predictions for the phase diagram of boson-boson mixtures based on our simulations of the two-component BEG model with a trapping potential. Although there are no available experimental data on boson-boson mixtures, we hope that our work can motivate further studies in this direction.

ACKNOWLEDGMENTS

We are grateful to K. Gubbels, H. van Beijeren, A. de Vries, and R. Movshovich for fruitful discussions and to J. de Graaf for technical help. This work was partially supported by the Netherlands Organization for Scientific Research (NWO).

-
- ¹E. H. Graf, D. M. Lee, and John D. Reppy, *Phys. Rev. Lett.* **19**, 417 (1967).
²M. Blume, V. J. Emery, and R. B. Griffiths, *Phys. Rev. A* **4**, 1071 (1971).
³A. Falicov and A. N. Berker, *Phys. Rev. Lett.* **74**, 426 (1995).
⁴M. Chan, N. Mulders, and J. Reppy, *Phys. Today* **49**(8), 30 (1996).
⁵M. Blume, *Phys. Rev.* **141**, 517 (1966); H. W. Capel, *Physica (Amsterdam)* **32**, 966 (1966).
⁶H. Ez-Zahraouy and A. Kassou-Ou-Ali, *Phys. Rev. B* **69**, 064415 (2004); H. Ez-Zahraouy, *Phys. Scr.* **51**, 310 (1995).
⁷M. Tanaka and T. Kawabe, *J. Phys. Soc. Jpn.* **54**, 2194 (1985).
⁸Yung-Li Wang, Felix Lee, and J. D. Kimel, *Phys. Rev. B* **36**, 8945 (1987).
⁹W. Selke, V. L. Pokrovsky, B. Büchner, and T. Kroll, *Eur. Phys. J. B* **30**, 83 (2002).
¹⁰U. Löw, V. J. Emery, K. Fabricius, and S. A. Kivelson, *Phys. Rev. Lett.* **72**, 1918 (1994).
¹¹J. D. Kimel, Per Arne Rikvold, and Yung-Li Wang, *Phys. Rev. B* **45**, 7237 (1992).
¹²O. Gygi, H. G. Katzgraber, M. Troyer, S. Wessel, and G. G. Batrouni, *Phys. Rev. A* **73**, 063606 (2006).
¹³H. Shishido, R. Settai, D. Aoki, S. Ikeda, H. Nakawaki, N. Kawamura, T. Iizuka, Y. Inada, K. Sugiyama, T. Takeuchi, K. Kindo, T. C. Kobayashi, Y. Haga, H. Harima, Y. Aoki, T. Namiki, H. Sato, and Y. Onuki, *J. Phys. Soc. Jpn.* **71**, 162 (2002).
¹⁴M. Nicklas, O. Stockert, Tuson Park, K. Habicht, K. Kiefer, L. D. Pham, J. D. Thompson, Z. Fisk, and F. Steglich, *Phys. Rev. B* **76**, 052401 (2007).
¹⁵L. D. Pham, Tuson Park, S. Maquilon, J. D. Thompson, and Z. Fisk, *Phys. Rev. Lett.* **97**, 056404 (2006).
¹⁶Tuson Park, F. Ronning, H. Q. Yuan, M. B. Salamon, R. Movshovich, J. L. Sarrao, and J. D. Thompson, *Nature (London)* **440**, 65 (2006).
¹⁷Martin W. Zwierlein, Christian H. Schunck, André Schirotzek, and Wolfgang Ketterle, *Nature (London)* **442**, 54 (2006).
¹⁸Guthrie B. Partridge, Wenhui Li, Ramsey I. Kamar, Yean-an Liao, and Randall G. Hulet, *Science* **311**, 503 (2006).
¹⁹K. B. Gubbels, M. W. J. Romans, and H. T. C. Stoof, *Phys. Rev. Lett.* **97**, 210402 (2006).
²⁰Yong-il Shin, Christian H. Schunck, André Schirotzek, and Wolfgang Ketterle, *Nature (London)* **451**, 689 (2008).
²¹C. Lobo, A. Recati, S. Giorgini, and S. Stringari, *Phys. Rev. Lett.* **97**, 200403 (2006).
²²K. B. Gubbels and H. T. C. Stoof, *Phys. Rev. Lett.* **100**, 140407 (2008).